Asian Journal of Chemistry; Vol. 35, No. 10 (2023), 2445-2450

ASIAN JOURNAL OF CHEMISTRY

https://doi.org/10.14233/ajchem.2023.28276

Spectroscopic and DFT Analysis of (*Z*)-3-(Anthracen-9-yl)-2-(naphthalen-1-yl)acrylonitrile Fluorophore

G. PRABHU[1], R. REVATHI[2], N. NAGARAJAN[3,*] and R. RENGANATHAN[1,*]

[1]School of Chemistry, Bharathidasan University, Tiruchirappalli-620024, India
[2]Department of Chemistry, Mahendra Arts and Science College (Autonomous), Kalippatti, Namakkal-637501, India
[3]Department of Basic Engineering, Government Polytechnic College, Keezhapalur, Ariyalur-621707, India

*Corresponding authors: E-mail: drnnrajan@gmail.com; rrengas@gmail.com

Received: 12 July 2023; *Accepted*: 9 August 2023; *Published online*: 28 September 2023; AJC-21395

Fluorophore molecule (*Z*)-3-(anthracen-9-yl)-2-(naphthalen-1-yl)acrylonitrile (ANCN) containing anthracene as donor (D), acrylonitrile as acceptor (A) and naphthalene as donor (D) has been synthesized and characterized. ANCN is crystallized in monoclinic crystal system with $P2_1/c$ space group. The absorption spectra of the compounds are dominated by intramolecular charge transitions that arise from the anthracene core to the acceptor groups. The compounds display distinct dual and single emission behaviour in different solvent environments. The CIE colour chromaticity diagram shows that the emission of ANCN in dichloromethane solution is in blue region, while neat film in greenish blue and 1% ANCN doped with PMMA in bluish-green region. Frontier molecular orbitals of the compound show that the localization of HOMO can be visualized on the anthracene unit and the LUMO is localized on the acrylonitrile unit. Thus, there is an intramolecular charge transfer (ICT) from HOMO to LUMO.

Keywords: (Naphthalen-1-yl)acrylonitrile fluorophore, Crystal structure, Optical properties, HOMO-LUMO and DFT analysis.

INTRODUCTION

An interest in spectroscopic properties of organic molecules featuring intramolecular charge transfer (ICT) has attracted increasing attention in both biochemistry and photochemistry, because of their notable applications in the field of molecular electronics, organic sensors, dye sensitized solar cells, non-linear optics and pharmacology [1-5]. In recent years, considerable attention has been focused on donor-acceptor-donor (D-A-D) system featuring ICT based on polycyclic aromatic hydrocarbons that are applicable in organic electronic devices such as organic light emitting diodes (OLEDs), organic light emitting transistors (OLETs), solid-state lighting (SSL), chemical sensors and photovoltaic cells [6-8].

Among the various polycyclic ring structures, anthracene and naphthalene are being utilized extensively, because these derivatives display intrinsically high thermal stability, tunable fluorescent wavelength and more adjustable charge transporting properties [9,10]. More importantly, anthracene moiety with its intrinsic planarity and grid structure, it can be easily modified at the 9,10-positions by incorporating various functionalized moieties. Continuous efforts have been put forward to analyze the effect of substituent on optical properties of various D-A-D groups with anthracene moiety [11-16]. However, despite this effort, the influence of different donor-acceptor substituents on its photophysical properties is not yet completely understood. Presumably, these groups are very sensitive to the solvent environments, which drastically changes its absorption and emission behaviour.

In view of this, the work presents the synthesis of (*Z*)-3-(anthracen-9-yl)-2-(naphthalen-1-yl)acrylonitrile [17] and were characterized using NMR, HR-MS and single crystal X-ray diffraction techniques. While their photophysical characteristics in fluids and polymer matrices have been researched to some extent, anthracene-based compounds have been the subject of far more research in the context of device development [18-21]. The photophysical characteristics of the molecule have been investigated in various media, such as solids, solutions and poly(methyl methacrylate) (PMMA) matrices. The DFT calculations were performed to elucidate the molecular electrostatic potential

surface and frontier molecular orbitals of the compound. This study will present a viable approach for acquiring high performance optoelectronic materials.

EXPERIMENTAL

Anthracene-9-carbaldehyde and poly(methyl methacrylate) (PMMA) with the average Mw of ~120,000 were purchased from Sigma-Aldrich, while naphthalen-1-yl-acetonitrile and sodium hydroxide (NaOH) were purchased from Spectrochem, India. Thin layer chromatography (TLC) precoated silica gel sheets obtained from Merck. Column chromatography was carried out by using (100-200) mesh silica gel as a stationary phase. All the solvents toluene, tetrahydrofuran, ethylacetate, acetonitrile, dichloromethane, N,N-dimethylformamide (DMF) and dimethyl sulfoxide (DMSO) used were of Analar reagent grade and used as received without further purification. The ^{1}H NMR (400 MHz) and ^{13}C NMR spectra (100 MHz) were recorded on a Bruker spectrometer in $CDCl_3$ solvent with tetramethylsilane as internal standard. High resolution mass spectra (HR-MS) were recorded with a MICRO-Q TOF mass spectrometer by using the ESI technique at 10 eV. Absorption and fluorescence spectral measurements were recorded by using JASCO V630 UV-visible spectrophotometer and JASCO FP-8300 spectrofluorimeter. Single-crystal X-ray data for ANCN were collected on a Bruker APEX-II CCD diffractometer. The single-crystal X-ray diffraction analysis for molecule (*Z*)-3-(anthracen-9-yl)-2-(naphthalen-1-yl)acrylonitrile (ANCN) was obtained by solvent diffusion method using hexane/ethyl acetate at 25 ºC (CCDC reference: 2259292). Theoretical calculation was optimized using the Gaussian 09W software package using DFT method at the B3LYP/6-31+G (d,p) level of theory.

General procedure: The desired compound was prepared as per the synthetic methodology given in **Scheme-I**. In a typical procedure, 50 mL round bottom flask was charged with anthracene-9-carbaldehyde (1 mmol) and naphthalen-1-yl-acetonitrile (1 mmol) were uniformly dispersed in ethanol (34 V) and the mixture was dissolved homogeneously. To a mixture 10% NaOH ethanolic solution was added and kept stirred for 12 h at room temperature. The progress of the reaction was monitored by TLC. After the completion of reaction, solvent was evaporated under reduced pressure and the residue was dissolved in ethyl acetate and washed with brine solution. The obtained compound was further purified using column chromatography (100-200 mesh silica gel) to afford the final product (*Z*)-3-(anthracen-9-yl)-2-(naphthalen-1-yl)acrylonitrile (ANCN). The obtained crystal was successfully grown from mixed hexane/ethyl acetate at room temperature and the structure was characterized by a single-crystal X-ray diffraction study. ^{1}H NMR (400 MHz, $CDCl_3$) δ ppm: 8.57 (s, 1H), 8.42 (d, J = 8.4 Hz, 1H), 8.28 (s, 1H), 8.23 (d, J = 0.8 Hz, 2H), 8.21 (d, J = 0.8 Hz, 2H), 8.10-8.02 (m, 2H), 7.98 (d, J = 8.4 Hz, 1H), 7.89-7.52 (m, 7H). ^{13}C NMR (100 MHz, $CDCl_3$) δ ppm: 146.5, 133.9, 132.7, 131.3, 130.8, 130.4, 129.4, 129.2, 129.15, 128.9, 127.6, 127.5, 126.9, 126.7, 125.6, 125.5, 124.9, 124.5, 120.3, 117.2. HR-MS (ESI) *m/z*: $C_{27}H_{17}N$ $[M+Na]^+$: 378.1258, found: 378.1232.

RESULTS AND DISCUSSION

Anthracene-9-carbaldehyde which undergoes Knoevenagel condensation with naphthalen-1-yl-acetonitrile in presence of 10% NaOH in ethanol to yield the target fluorophore molecule (*Z*)-3-(anthracen-9-yl)-2-(naphthalen-1-yl)acrylonitrile (ANCN). The chemical structure of the ANCN final product was well characterized by ^{1}H NMR, ^{13}C NMR and HR-MS spectroscopic techniques.

The compound ANCN crystallized from the mixed solvents hexane/ethyl acetate at room temperature in the monoclinic crystal system with $P2_1/c$ space group. The molecular structure of ANCN is illustrated in Fig. 1 & Table-1; and the selected bond lengths and bond angles are given in Table-2. The ANCN compound consists of an anthracene ring linked to naphthalene ring *via* acrylonitrile unit, representing a D-A-D system. The molecular structure of the synthesized ANCN acrylonitrile fluorophore crystal was optimized using the Gaussian 09W [22] software package using DFT method at the B3LYP/6-31+G (d,p) [23-25] level of theory. The optimized structure has two different ring structures, the anthracene unit and the naph-

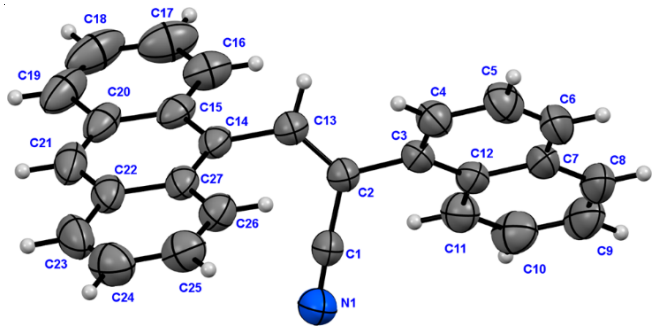

Fig. 1. ORTEP structural drawing of ANCN with ellipsoids shown at the 30% probability level

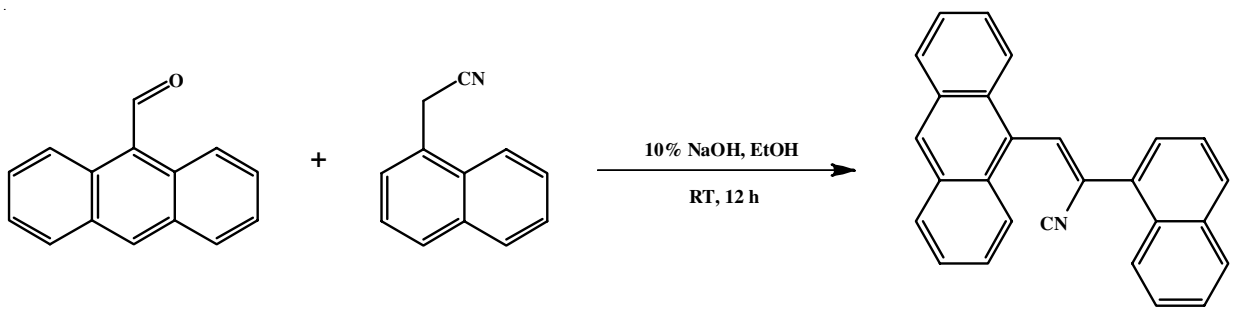

Scheme-I: Synthesis of the ANCN fluorophore. Reaction conditions: i) 10% NaOH, EtOH, RT, 12 h

TABLE-1
CRYSTALLOGRAPHIC DATA OF ANCN

Chemical formula	$C_{27}H_{17}N$
M_r	355.42
Crystal system, space group	Monoclinic, $P2_1/c$
Temperature (K)	298
a, *b*, *c* (Å)	7.6533 (5), 23.0165 (16), 12.9567 (10)
β (°)	105.703 (3)
V (Å^3)	2197.2 (3)
Z	4
Radiation type	Mo*K*α
μ (mm^{-1})	0.06
Crystal size (mm)	0.31 × 0.27 × 0.23
Data collection	
Diffractometer	Bruker D8 Quest XRD
Absorption correction	Multi-scan
T_{min}, T_{max}	0.713, 0.746
No. of measured, independent and observed [I > 2σ(I)] reflections	72798, 6436, 4118
R_{int}	0.050
$(\sin \theta/\lambda)_{max}$ (Å^{-1})	0.706
Refinement	
R[F^2 > 2σ(F^2)], wR(F^2), S	0.096, 0.366, 1.37
No. of reflections	6436
No. of parameters	253
H-atom treatment	H-atom parameters constrained
$(\Delta/\sigma)_{max}$	0.124
$\Delta\rho_{max}$, $\Delta\rho_{min}$ (e Å^{-3})	1.16, -0.37

thalene unit, which are resided in two different planes similar to the observation in their crystal structure (Fig. 2). This can be further affirmed by the C23-C21-C3-C4 dihedral angle, which is -176.250.

The geometrical parameters of the optimized crystal structure correlates well with the experimental crystal values. This can be observed through the various bond parameters as given in Table-2. For instance, the C2-C3 bond length of the optimized structure of ANCN acrylonitrile fluorophore is 1.439 Å and the crystal structure bond length is 1.435 Å. Moreover, the C3-C4-C5 bond angle of 118.37º in the optimized structure is comparable with the C3-C4-C5 bond angle of 118.25º in the crystal structure. The dihedral angle C24-C23-C21-C3 of the optimized structure exhibits a value of -120.51º, while the corresponding angle in the crystal structure was calculated at -121.28º.

TABLE-2
BOND PARAMETERS OF OPTIMIZED GEOMETRY AND CRYSTAL STRUCTURE OF ANCN

S. No.	Bond parameters	Optimized geometry	Crystal structure
A	Bond length (Å)		
1	C2–C3	1.439	1.435
2	C3–C21	1.356	1.348
3	C21–C23	1.479	1.473
4	C3–C4	1.496	1.490
5	N1–C2	1.165	1.150
B	Bond angle (°)		
1	C23–C21–C3	128.14	127.21
2	C21–C3–C2	120.83	119.48
3	C2–C3–C4	117.39	117.35
4	C3–C4–C5	118.37	118.25
C	Dihedral angle (°)		
1	C24–C23–C21–C3	-120.51	-121.68
2	C23–C21–C3–C2	2.18	4.39
3	C23–C21–C3–C4	-176.25	-171.97
4	C2–C3–C4–C5	-122.64	-125.20
5	C2–C3–C4–C20	57.78	53.05

Photophysical analysis: The ground state absorption and excited state emission characteristics of ANCN in solvents of varying polarity were measured and the respective spectra are displayed in Fig. 3a-c and the relevant data are shown in Table-3. ANCN displays two distinct absorption characteristics in which the first band is located in the shorter wavelength region of 230 to 280 nm possessing higher a molar extinction coefficient in the range of 1.19×10^4 M^{-1} cm^{-1} that attributed to the π-π* transitions occurring in the anthracene and naphthalene donor units.

On the other hand, the second absorption band located in the longer wavelength region of 350 to 430 nm with lowered molar extinction coefficient in the range of 1.22×10^3 M^{-1} cm^{-1} corresponds to the intramolecular charge transfer characteristics from the donor unit to the acrylonitrile acceptor unit. The optical energy gaps (E_g) obtained from the onset of the absorption spectrum in various solvents lie in the range of 3.18 eV. In general, ANCN possess three emission bands in which the first two bands with higher emission intensity are observed in the region of 390-480 nm with peak maximum lies around 400 and 431 nm, while the third emission observed as shoulder band in the region of 510-600 nm. Among these three emission

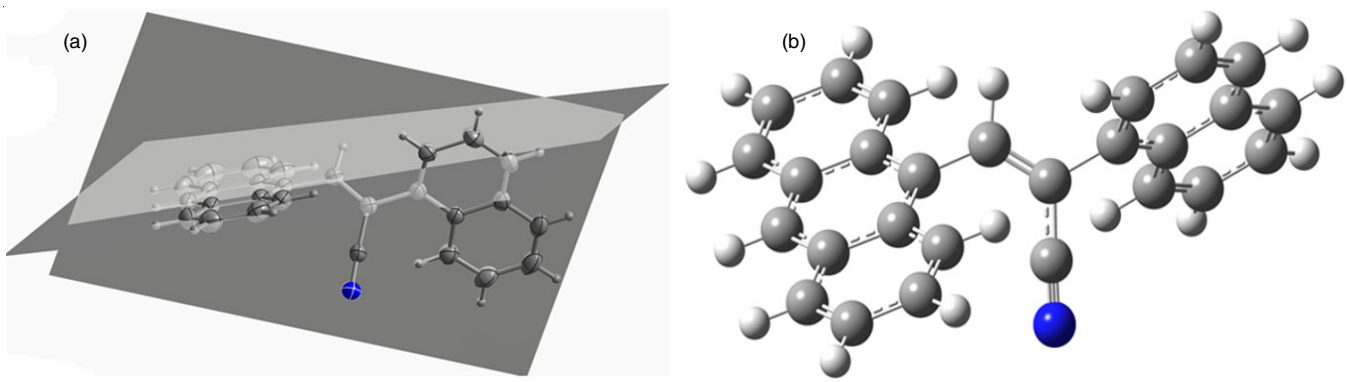

Fig. 2. (a) A representation of the anthracene unit and the naphthalene unit residing in different planes and (b) the optimized structure using DFT method at the B3LYP/6-31G + (d,p) level

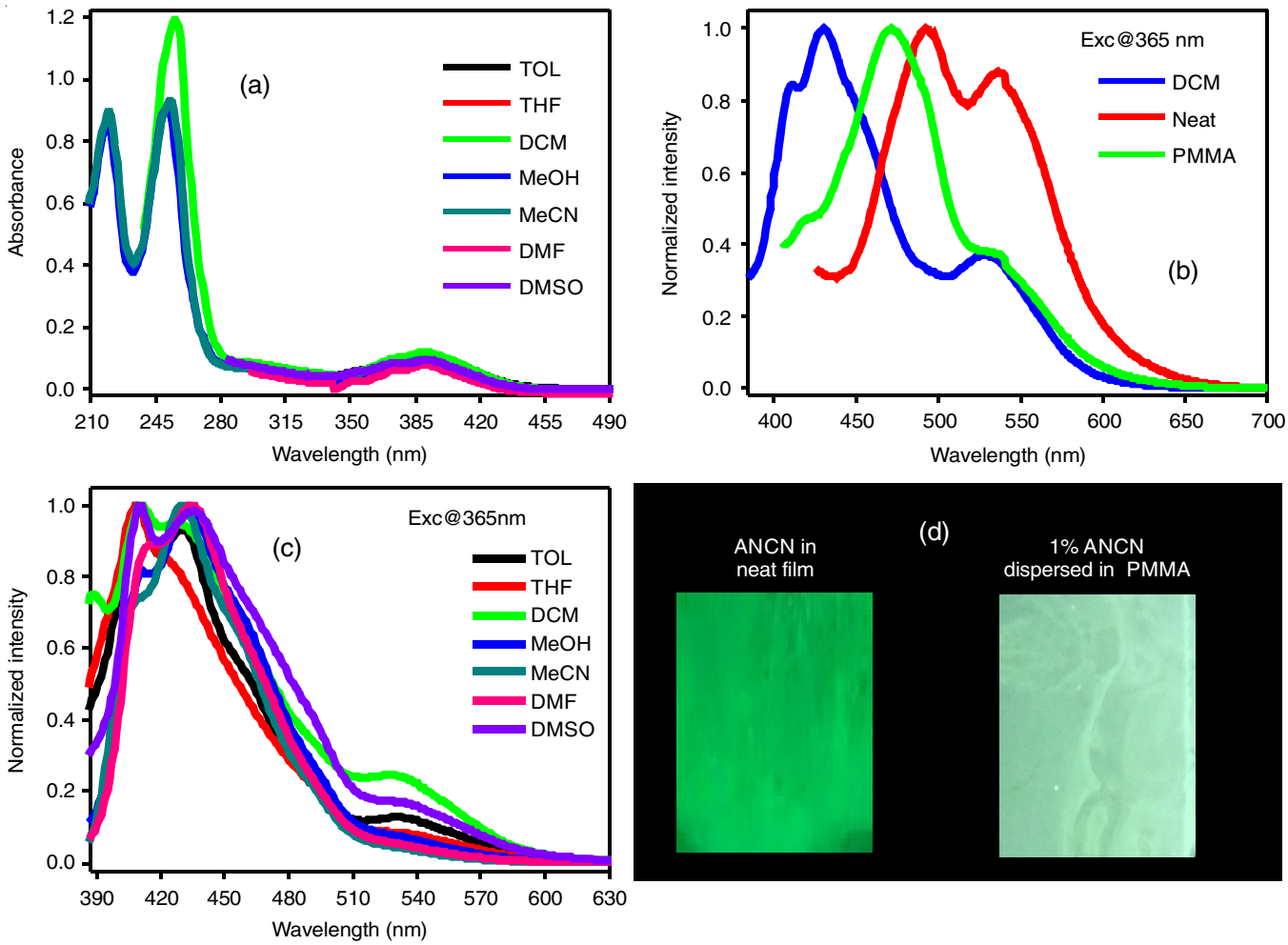

Fig. 3. (a) Absorption spectrum of ANCN in different solvents, (b) Emission spectra of ANCN in DCM, neat film and 1% ANCN dispersed in PMMA, (c) Emission spectrum of ANCN excited at 365 nm in different solvents, (d) The photographs of the neat film and 1% ANCN dispersed in PMMA states excited at 365 nm UV illumination

TABLE-3
PHOTOPHYSICAL DATA OF ANCN IN VARIOUS SOLVENTS

	TOL	THF	DCM	MeOH	CH_3CN	DMF	DMSO	Neat film	1% ANCN in PMMA
[a]λ_{abs} (nm) [ε (mol^{-1} cm^{-1})]	302 [7,237] 391 [11,172]	389 [9,568]	256 [119,110] 390 [12,244]	251 [90,602] 366 [6,036] 387 [8,710]	253 [93,266] 371 [8,062] 387 [9,470]	352 [2,772] 390 [7,953]	374 [8,305] 392 [9,532]		
[b]λ_{emi} (nm) Ex@365 nm	409 430 531	409 530	431 530	433 530	430 530	416 530	410 435 528	492 536	472 529

[a]Absorption wavelength λ_{abs} (nm) and Molar extinction Coefficient [ε (mol^{-1} cm^{-1})] of ANCN in different solvents (1×10^{-5} M).
[b]Emission wavelength λ_{emi} (nm) of ANCN excited at 365 nm in different solvents (1×10^{-5} M), neat film and 1% ANCN dispersed in PMMA.

bands, the shoulder band is observed with all solvents while either one of the first two emission bands were observed with varying solvents despite all three emission bands observed in toluene and DMSO medium. In contrast to the solution state characteristics of ANCN, the emission characteristics of ANCN was varied significantly in the solid-state conditions (Fig. 3b,c). For instance, ANCN in the neat film exhibited an emission in the range of 430-650 nm with a peak maximum located at 492 and 536 nm, which is red-shifted by 61 nm compared to its emission characteristics in the DCM solvent medium. Dispersing 1% ANCN in PMMA blue-shifted the emission peak by 20 nm compared with its neat film medium. The emission spectra of ANCN molecule in the neat-film show an obviously broader peak and slight red-shift of the peak compared to the emission spectra of ANCN in CH_2Cl_2 solution and 1% ANCN in PMMA film. These phenomena imply that the emitter reported herein

form a compact stacking structure in the thin film that benefits charge transport. The peak maximum of the 1% ANCN in PMMA film emission is found to be observed at 472 nm and another shoulder band around 529 nm. The intermolecular interactions between the ANCN molecules are likely to be stronger in the highly concentrated solid state than those in less concentrated solution states (1×10^{-5} M) that led to the observed different photophysical properties between these two states. The observed promising luminescence characteristics of the ANCN reveal it as a potential candidate in light emitting applications such as organic light emitting diodes (OLEDs) and organic light emitting transistors (OLETs).

CIE colour chromaticity: The photoluminescence spectra at 365 nm of ANCN in DCM, neat film and 1% ANCN in PMMA have the corresponding chromaticity coordinates as follows: DCM ($x = 0.1803$; $y = 0.1918$); neat film ($x = 0.2484$; $y = 0.4263$) and 1% ANCN in PMMA ($x = 0.1765$; $y = 0.2459$), respectively. The emission of PL spectra for DCM in the blue region, while neat film in greenish-blue and 1% ANCN doped with PMMA in bluish-green region. The results are shown in the CIE colour chromaticity diagram as presented in Fig. 4.

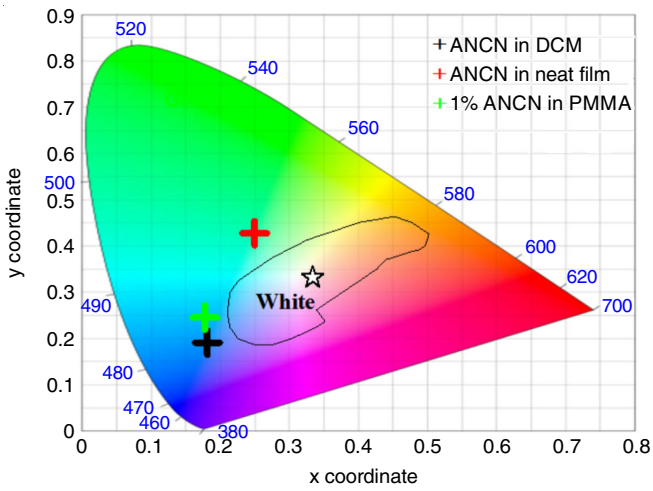

Fig. 4. CIE colour chromaticity diagram of the compound

Molecular electrostatic potential (MEP): The molecular electrostatic potential surface is shown in Fig. 5. The red coloured areas on the molecule depict the more electron-rich areas with negative potential. Also, the green coloured areas illustrate the neutral regions with zero potential. The blue coloured areas show electron deficient regions with positive potential [26]. It is clear that the N atom attached to C2-C3-C21 which is connecting both the anthracene unit and naphthalene unit shows red coloured surface because of the more electronegativity nature of the N-atom. Therefore, this region is electron rich region. Moreover, the anthracene and naphthalene units have green surface over them. Thus, both of these units are neutral with zero potential. No blue regions are observed in this molecule and thus the molecule does not have any electron deficient regions.

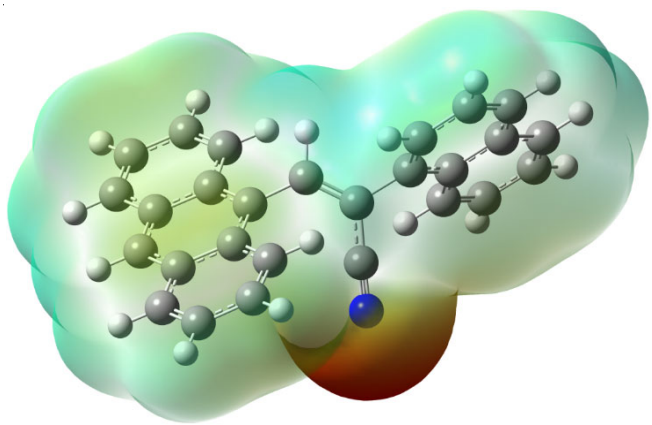

Fig. 5. Molecular electrostatic surface of ANCN fluorophore

Frontier molecular orbital (FMO) analysis: Frontier molecular orbitals (HOMO) and (LUMO), obtained from the B3LYP/6-31G+(d,p) level of calculation are shown in Fig. 6a. The localization of HOMO can be visualized on the anthracene unit and the LUMO is localized on the acrylonitrile unit. Thus, there is an intramolecular charge transfer (ICT) from HOMO to LUMO. Also, HOMO-1 is localized on the naphthalene unit

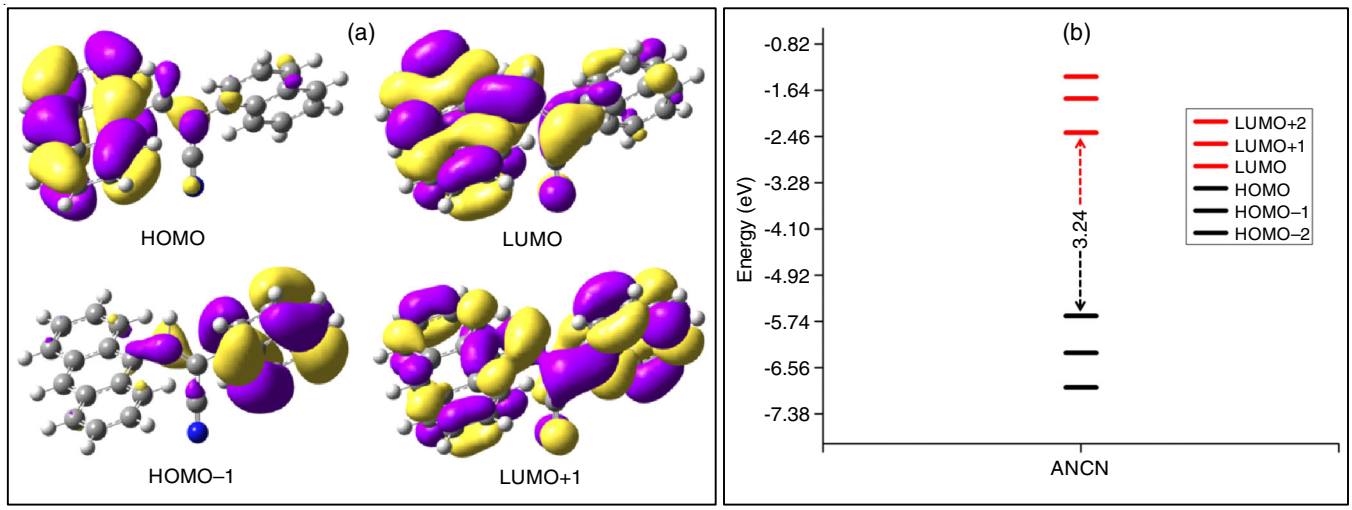

Fig. 6. (a) Frontier molecular orbitals (HOMO and LUMO) of ANCN fluorophore obtained from DFT calculations, (b) HOMO and LUMO energy gap (eV) of ANCN fluorophore

whereas the LUMO+1 is completely localized on the whole molecule. Therefore, the transition from HOMO-1 to LUMO or LUMO+1 shows ICT. Similarly, the transition from HOMO to LUMO+1 also shows ICT. The HOMO-2, HOMO-1, HOMO, LUMO, LUMO+1 and LUMO+2 energies are depicted Fig. 6b. The HOMO-LUMO gap for ANCN is calculated to be 3.24 eV, which lies close enough with the experimentally calculated value of 3.18 eV obtained from the UV-vis analysis.

Conclusion

In this work, D-A-D kind fluorescent emitter molecule ANCN containing anthracene, acrylonitrile and naphthalene respectively, has been synthesized and characterized thoroughly using NMR, HR-MS and single crystal X-ray diffraction measurements. Twisted orientation of anthracene and naphthalene unit has been found from crystal structure. The compound show moderate solvatochromic behaviour in various solvents with different polarity and show profound intensity enhanced emission. Broadened emission due to molecular interaction in solid state has been further confirmed by CIE colour chromaticity analysis. The DFT studies reveal that there is an intramolecular charge transfer between anthracene and acrylonitrile unit. Overall, the studied photophysical properties of anthracene derivatives are of vast significance in the further development of novel molecules that will find extensive applications in research fields of current interests.

ACKNOWLEDGEMENTS

One of the authors, G.P. acknowledges the fellowship received through the UGC-BSR-RFSMS (F.4-1/2006 (BSR)/7-22/2007(BSR) dated 22.10.2013) for the financial assistant. Another author, R.R. thanks DST-Nanomission (Ref. No. SR/NM/NS-1256/2013) and UGC (UGC-2013-35169/2015) for research funding and UGC (Ref. No. F.6-6/2016-17/EMERITUS-2015-17-OBC-7855/(SA-II)) for the award of Emeritus Fellowship. Thanks are also due to DST-FIST for instrument facilities at School of Chemistry, Bharathidasan University and Dr. R. Vijay Solomon, Department of Chemistry, Madras Christian College (Autonomous) for providing the DFT analysis. Finally, third author, N.N. also thanks Government Polytechnic College, Keezhapalur, Tamil Nadu and Directorate of Technical Education, Tamil Nadu, India for providing the infrastructure research facilities.

CONFLICT OF INTEREST

The authors declare that there is no conflict of interests regarding the publication of this article.

REFERENCES

1. E. Romero, V.I. Novoderezhkin and R. van Grondelle, *Nature*, **543**, 355 (2017); https://doi.org/10.1038/nature22012
2. K. Wu, J. Chen, J.R. McBride and T. Lian, *Science*, **349**, 632 (2015); https://doi.org/10.1126/science.aac5443
3. H. Park, H. Kim, G. Moon and W. Choi, *Energy Environ. Sci.*, **9**, 411 (2016); https://doi.org/10.1039/C5EE02575C
4. W. Chi, J. Chen, W. Liu, C. Wang, Q. Qi, Q. Qiao, T.M. Tan, K. Xiong, X. Liu, K. Kang, Y.-T. Chang, Z. Xu and X. Liu, *J. Am. Chem. Soc.*, **142**, 6777 (2020); https://doi.org/10.1021/jacs.0c01473
5. W. Chi, Q. Qiao, R. Lee, W. Liu, Y.S. Teo, D. Gu, M.J. Lang, Y.T. Chang, Z. Xu and X. Liu, *Angew. Chem. Int. Ed.*, **58**, 7073 (2019); https://doi.org/10.1002/anie.201902766
6. J. Zou, Z. Yin, P. Wang, D. Chen, J. Shao, Q. Zhang, L. Sun, W. Huang and X. Dong, *Chem. Sci.*, **9**, 2188 (2018); https://doi.org/10.1039/C7SC04694D
7. P. Hao, Y. Xu, J. Shen and Y. Fu, *Dyes Pigments*, **186**, 108941 (2021); https://doi.org/10.1016/j.dyepig.2020.108941
8. A. Nitti, M. Signorile, M. Boiocchi, G. Bianchi, R. Po and D. Pasini, *J. Org. Chem.*, **81**, 11035 (2016); https://doi.org/10.1021/acs.joc.6b01922
9. A. Nitti, G. Bianchi, R. Po, T.M. Swager and D. Pasini, *J. Am. Chem. Soc.*, **139**, 8788 (2017); https://doi.org/10.1021/jacs.7b03412
10. A. Nitti, P. Osw, G. Calcagno, C. Botta, S.I. Etkind, G. Bianchi, R. Po, T.M. Swager and D. Pasini, *Org. Lett.*, **22**, 3263 (2020); https://doi.org/10.1021/acs.orglett.0c01043
11. P. Osw, A. Nitti, M.N. Abdullah, S.I. Etkind, J. Mwaura, A. Galbiati and D. Pasini, *Polymers*, **12**, 720 (2020); https://doi.org/10.3390/polym12030720
12. R. Malatong, C. Kaiyasuan, P. Nalaoh, S. Jungsuttiwong, T. Sudyoadsuk and V. Promarak, *Dyes Pigments*, **184**, 108874 (2021); https://doi.org/10.1016/j.dyepig.2020.108874
13. J. Huang, J.H. Su and H. Tian, *J. Mater. Chem.*, **22**, 10977 (2012); https://doi.org/10.1039/c2jm16855c
14. J. Shi and C.W. Tang, *Appl. Phys. Lett.*, **80**, 3201 (2002); https://doi.org/10.1063/1.1475361
15. Y.H. Kim, H.C. Jeong, S.H. Kim, K. Yang and S.K. Kwon, *Adv. Funct. Mater.*, **15**, 1799 (2005); https://doi.org/10.1002/adfm.200500051
16. M.T. Lee, H.H. Chen, C.H. Liao, C.H. Tsai and C.H. Chen, *Appl. Phys. Lett.*, **85**, 3301 (2004); https://doi.org/10.1063/1.1804232
17. N.P. Buu-Hoi and N. Hoan, *J. Org. Chem.*, **16**, 874 (1951); https://doi.org/10.1021/jo01146a007
18. C.J. Zheng, W.M. Zhao, Z.Q. Wang, D. Huang, J. Ye, X.M. Ou, X.-H. Zhang, C.-S. Lee and S.-T. Lee, *J. Mater. Chem.*, **20**, 1560 (2010); https://doi.org/10.1039/b918739a
19. J.Y. Hu, Y.J. Pu, F. Satoh, S. Kawata, H. Katagiri, H. Sasabe and J. Kido, *Adv. Funct. Mater.*, **24**, 2064 (2014); https://doi.org/10.1002/adfm.201302907
20. J.S. Huh, Y.H. Ha, S.K. Kwon, Y.H. Kim and J.J. Kim, *ACS Appl. Mater. Interfaces*, **12**, 15422 (2020); https://doi.org/10.1021/acsami.9b21143
21. Y. Matsuo, H. Okada, Y. Kondo, I. Jeon, H. Wang, Y. Yu, T. Matsushita, M. Yanai and T. Ikuta, *ACS Appl. Mater. Interfaces*, **10**, 11810 (2018); https://doi.org/10.1021/acsami.8b00603
22. M.J. Frisch, G.W. Trucks, H.B. Schlegel, G.E. Scuseria, M.A. Robb, J.R. Cheeseman, G. Scalmani, V. Barone, B. Mennucci, G.A. Petersson, H. Na katsuji, M. Caricato, X. Li, H.P. Hratchian, A.F. Izmaylov, J. Bloino, G. Zheng, J.L. Sonnenberg, M. Hada, M. Ehara, K. Toyota, R. Fukuda, J. Hasegawa, M. Ishida, T. Nakajima, Y. Honda, O. Kitao, H. Nakai, T. Vreven, J.A. Montgomery Jr., J.E. Peralta, F. Ogliaro, M. Bearpark, J.J. Heyd, E. Brothers, K.N. Kudin, V.N. Staroverov, T. Keith, R. Kobayashi, J. Normand, K. Raghavachari, A. Rendell, J.C. Burant, S.S. Iyengar, J. Tomasi, M. Cossi, N. Rega, J.M. Millam, M. Klene, J. E. Knox, J.B. Cross, V. Bakken, C. Adamo, J. Jaramillo, R. Gomperts, R.E. Stratmann, O. Yazyev, A.J. Austin, R. Cammi, C. Pomelli, J.W. Ochterski, R.L. Martin, K. Morokuma, V.G. Zakrzewski, G.A. Voth, P. Salvador, J.J. Dannenberg, S. Dapprich, A.D. Daniels, O. Farkas, J.B. Foresman, J.V. Ortiz, J. Cioslowski and D.J. Fox, GAUSSIAN 09, revision B.01.; Gaussian Inc.: Wallingford, CT (2009).
23. V. Saheb and I. Sheikhshoaie, *Spectrochim. Acta A Mol. Biomol. Spectrosc.*, **81**, 144 (2011); https://doi.org/10.1016/j.saa.2011.05.080
24. A. Ramalingam, S. Kansiz, N. Dege and S. Sambandam, *J. Chem. Crystallogr.*, **51**, 273 (2021); https://doi.org/10.1007/s10870-020-00852-3
25. R.V. Solomon, P. Veerapandian, S.A. Vedha and P. Venuvanalingam, *J. Phys. Chem. A*, **116**, 4667 (2012); https://doi.org/10.1021/jp302276w
26. J.G. Samuel, B. Malgija, C. Ebenezer and R.V. Solomon, *Struct. Chem.*, **34**, 1289 (2023); https://doi.org/10.1007/s11224-022-02076-x